Complete Manuscript

Resistive Switching Characteristics of Integrated Polycrystalline HfO_2 based1T1R Devices

Hee-Dong Kim[*,1], Felice Crupi[2], Mindaugas Lukosius[3], Andreas Trusch[3], Christian Walczyk[3], Christian Wenger[**,3]

[1]Department of Electrical Engineering, Sejong University, Neungdong-ro 209, Gwangjin-gu, Seoul 143-747, Korea
[2]Dipartimento di Ingegneria Informatica, Modellistica, Elettronica e Sistemistica, Università della Calabria Via P. Bucci, 42C I-87036 Rende (CS), Italy
[3]IHP GmbH- Leibniz Institute for innovative microelectronics, Im Technologiepark 25, Frankfurt (Oder) 15236, Germany

Received ZZZ, revised ZZZ, accepted ZZZ
Published online ZZZ (Dates will be provided by the publisher.)
Keywords resistive switching memory, polycrystalline HfO_2, 1T1R, atomic vapor deposition

----

*Corresponding author: e-mail khd0708@sejong.ac.kr
**Corresponding author: e-mail wenger@ihp-microelectronics.com

In this work, bipolar resistive switching (RS) characteristics of polycrystalline hafnium oxide were studied for embedded 1T1R RRAM device applications. The HfO_2 films with thickness of 15 nm to 25 nm were grown by the atomic vapor deposition (AVD) method at 400 °C. The HfO_2 films were estimated as polycrystalline from the surface topography results by applying atomic force microscopy (AFM) and X-ray diffraction (XRD), and grain size observed in the AFM images increased when increasing thickness of HfO_2 films. In addition, current-voltage characteristics of the films were investigated to examine the RS characteristics. First, in the forming procedure, we observed the lowest forming voltage for 15 nm thick HfO_2 films and the forming voltage gradually increased with increasing the thickness of the HfO_2 films. A reproducible resistance switching behavior was observed with resistance ratio of ~20 and dc cycling of 100 times. SET and RESET voltages were measured about 1.2 and 1.6 V, respectively, indicating that the RRAM device can be operated below 2 V. The Current-Voltage characteristics are discussed in the frame of the quantum point contact model.

1 Introduction Resistive random access memories (RRAMs) with 1 transistor-1 resistor (1T1R) structures have been studied for embedded and high density nonvolatile memory (NVMs) applications. Compared to conventional flash memory [1], it has some advantage in the simplicity, low-power operation, high speed, and scalability. Moreover, embedded NVMs when employing the RRAM technology are of interest for many different system-on-chip (SoC) applications in Si-based complementary metal oxide semiconductor (CMOS) technologies, in particular for various wireless sensor networks (WSNs) and medical health care devices, since it is easy to reduce the power dissipation as a function of time in the inactive mode (standby) of the sensor node [2],[3]. Up to now, various kinds of resistive switching materials, i.e., metal-oxides [4],[5] and metal-nitrides [6],[7] have been explored to improve their resistive switching characteristics and reliability. Among them, hafnium oxide (HfO_2), which has been intensively studied as gate dielectric replacing SiO_2 in CMOS transistors, is suggested as one of the most promising candidates for RRAM devices due of its compatibility with the current process of semiconductor fabrication. However, most studies in RRAM researches have been focused on improving the performance and understanding the unclear RS mechanism, rather than a consideration of current semiconductor processing environment, by using physical vapor deposition (PVD). For this reason, the HfO_2 RRAM fabricated by atomic layer deposition (ALD) have been employing and studying to realize fab friendly devices [8],[9].

In addition, in order to fabricate RRAM devices in a manufacturing level, it is required to employ more cost competitive deposition method in terms of mass production than the single wafer ALD method for the deposition of the HfO_2 films. As a result, to satisfy reliability of both bottom electrodes and the HfO_2 films especially for the nanoscale

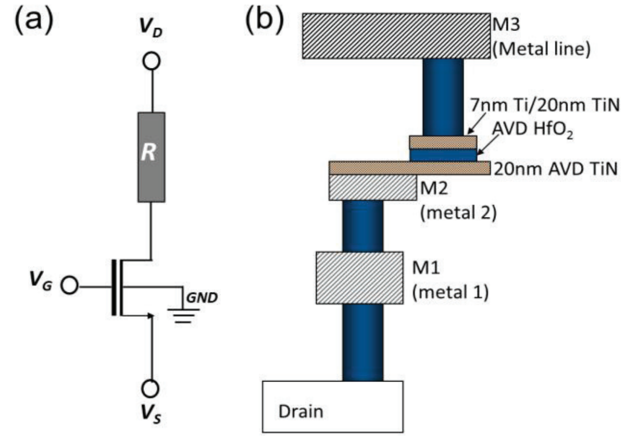

Figure 1 (a) Equivalent circuits of fabricated HfO_2-based 1T1R RRAM cells and (b) schematic of RRAM devices with AVD TiN bottom and AVD HfO_2 films on drain.

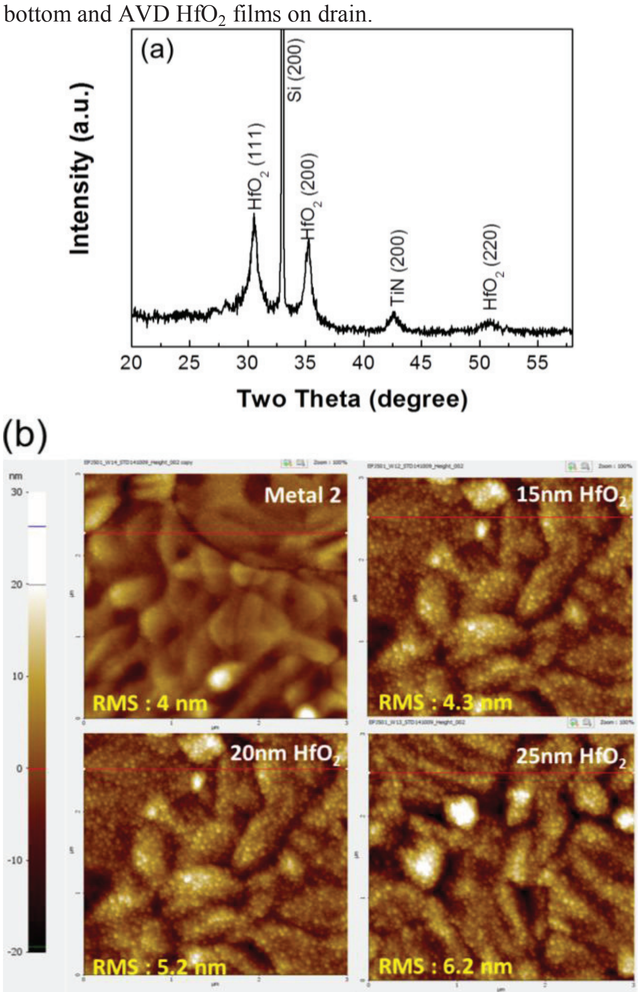

Figure 2 (a) XRD peaks for AVD HfO_2 films deposited at 400 °C and (b) AFM topography measured on metal 2 (i.e., AVD TiN BEs), 15 nm AVD HfO_2 films, 20 nm AVD HfO_2 films, and 25 nm HfO_2 films. This figure also shows their root mean square (RMS) properties.

and 3D structure memory applications, it is considered to study on chemical deposition method, i.e., atomic vapor deposition (AVD). Therefore, we have investigated the resistance switching behaviors of AVD grown HfO_2 films.

In this work, resistive switching characteristics of 1T1R devices with different thickness of AVD grown HfO_2 films were continually investigated. In addition, to study the conduction mechanism of the resistive switching behaviors, the current-voltage (*I–V*) characteristics have are discussed by applying the Quantum Point Contact (QPC) model [10], [13].

2 Experimental Procedure We firstly fabricated NMOS transistors as a selecting element. After that, featuring width (W) of 1.14 µm and length (L) of 0.24 µm, the resistive switching cell of metal-insulator-metal (MIM) is placed between the metallization levels 2 and 3, as illustrated in Fig. 1(b). In order to study the impact of the bottom electrode deposition process, an additional AVD TiN with thickness of 20 nm was deposited on top of the metal 2 stack. In addition, in order to study thickness dependence, HfO_2 films with thickness of 15 nm to 25 nm were deposited at 400 °C by using AVD method, respectively. Finally, HfO_2 was capped by 7 nm ionized metal plasma (IMP) Ti and 20 nm PVD TiN [11]. We measured the electrical properties of the memory cells using a Keithley 4200-SCS and Cascade PA200 Semi-automatic Probe System.

3 Results and discussions First, in order to check structural property of HfO_2 films deposited at 400 °C, we measured the X-ray diffraction peaks. Figure 2(a) reveals that the HfO_2 films deposited by AVD method at 400 °C have a polycrystalline monoclinic structure; the marked diffraction peak observed at ~30.5, 35.2, and 50.8° corresponding to (111), (200), and (220) planes originates in the scanned range of 20−55°.

Then, as shown in Fig. 2(b), we investigated roughness properties of the HfO_2 films by using atomic force microscope (AFM) in a non-contact mode with scanning range of 3um x 3um. As a result, it is found that the R_q (root mean squared) is gradually increased by increasing thickness of the HfO_2 films.

In forming process, a lower leakage is observed in thicker films and forming voltage is also gradually increased when increasing film's thickness, as shown in Fig. 3(a).

In set process of Fig. 3(b), we observed similar set voltage at around 1 V to around 1.5 V in all samples, while a current level at high resistive state (HRS) for a thicker sample, i.e., 25 nm AVD HfO_2 films, is lower than those of thinner samples, i.e., 15 nm and 20 nm AVD HfO_2 films. Then, a current ratio between set and reset is slightly increased with increasing thickness of the HfO_2 films in this study.

In Fig. 3(c), reset process for three samples shows a similar trend to set process in current level, while reset voltage is proportional in this test; especially, compared to 15 nm and 20 nm AVD HfO_2 films, reset voltage of 25 nm

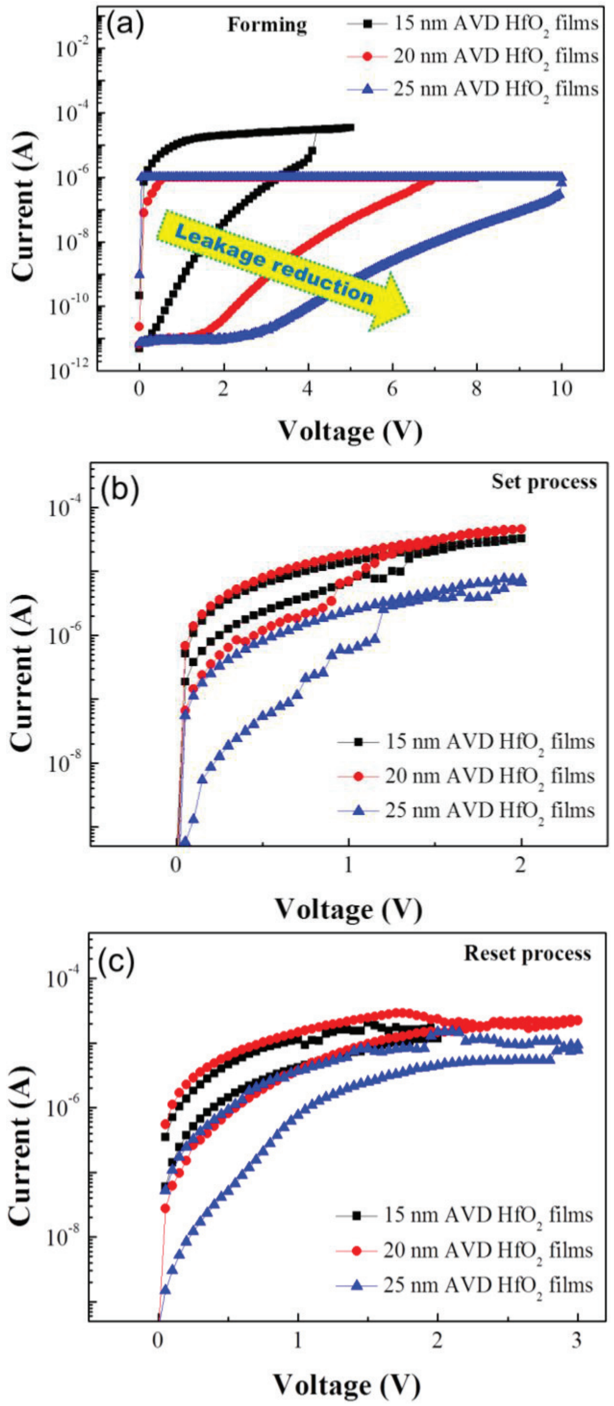

Figure 3 (a) Forming, (b) SET and (c) RESET characteristics for AVD HfO_2 based 1T1R RRAM with different thickness of 15 nm, 20 nm, and 25 nm HfO_2 films.

AVD HfO_2 films is observed over 1 V, i.e., from around 1.7 V to around 2.7 V.

$$I \approx \frac{2e}{h}\left\{ eV + \frac{1}{\alpha}\ln\left[\frac{1+\exp\left\{\alpha\left[\Phi_B - \frac{eV}{2}\right]\right\}}{1+\exp\left\{\alpha\left[\Phi_B + \frac{eV}{2}\right]\right\}}\right]\right\} \tag{1}$$

$$t_B = \frac{h\alpha}{2\pi^2}\sqrt{\frac{2\Phi_B}{m^*}} \tag{2}$$

$$r_B = \frac{hz_o}{2\pi\sqrt{2m^*\Phi_B}} \tag{3}$$

where Φ_B is the barrier height, α is a shape parameter related to the barrier thickness t_B, e is the electron charge, h is the Planck's constant m^* is the electron effective mass in the constriction (assumed equal to $0.44m_0$, where m_0 is the free electron rest mass), r_B is the constriction radius at the narrowest point and z_0=2.404 is the first zero of the Bessel function J_0.

where Φ_B is the barrier height, α is a shape parameter related to the barrier thickness t_B, e is the electron charge, h is the Planck's constant m^* is the electron effective mass in the constriction (assumed equal to $0.44m_0$, where m_0 is the free electron rest mass), r_B is the constriction radius at the narrowest point and z_0=2.404 is the first zero of the Bessel function J_0.

As shown in Fig. 4 and 5, the QPC model accurately reproduces typical *I–V* curves of the high resistive state (HRS) as well of the low resistive state (LRS). By comparing the fitting parameters for the two states, we observe that the conduction in the HRS is ruled by a higher and larger potential barrier with respect to the LRS (Φ_B = 1.53 eV and t_B = 0.47 nm for the HRS, Φ_B = 0.97 eV and t_B = 0.32 nm for the LRS). The values of the constriction radius lower than 1 nm (r_B = 0.57 nm for the HRS, and r_B = 0.72 nm for the LRS) confirms the high potential scalability of the resistive RRAMs and the necessity of using a quantum model for explaining the conduction mechanism through the filamentary path.

Finally, in order to estimate device's reliability, we have investigated the dc-cycling characteristics at reading voltage (V_{READ}) of 0.1 V. As shown in Fig. 6, we have successfully done a repetitive resistive switching for 100 times in dc mode.

4 Conclusion In this study, we have successfully demonstrated bipolar resistive switching (RS) characteristics of 15 nm polycrystalline HfO_2 films and TiN BEs using atomic vapor deposition (AVD) method at 400 °C. In forming, the forming voltage is gradually increased with increasing the thickness of the HfO_2 films. The QPC model allows to accurately reproduce the I-V curves for both resistance states and to estimate the basic physical parameters of the filamentary path. The constriction radius is lower than 1 nm for both resistance states, thus confirming the high potential scalability of RRAMs. A reproducible resis

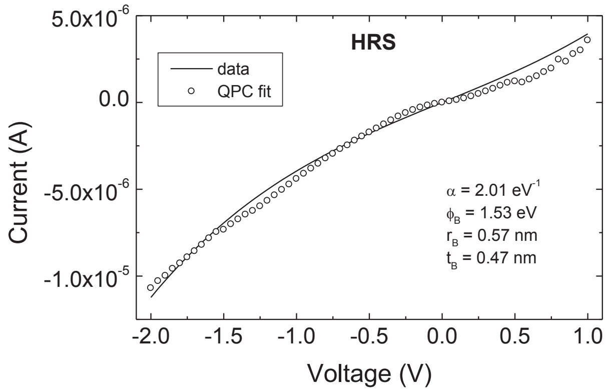

Figure 4 Experimental and theoretical I-V characteristics for the HRS. The QPC model (Eq. (1)) was used for the theoretical curve.

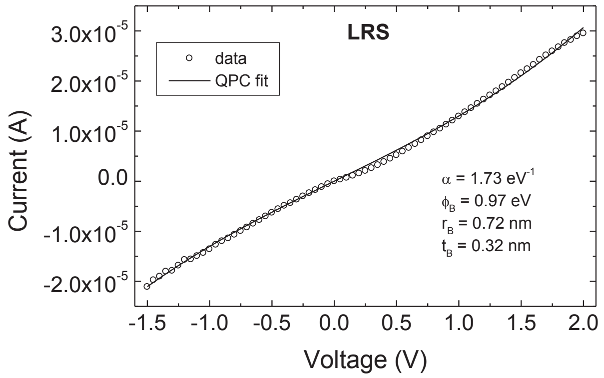

Figure 5 Experimental and theoretical I-V characteristics for the LRS. The QPC model (Eq. (1)) was used for the theoretical curve.

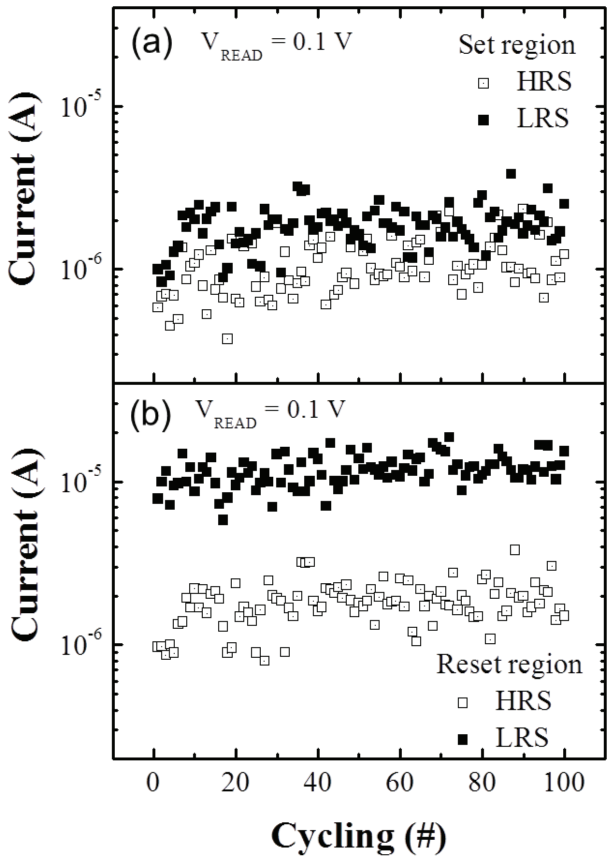

Figure 4 The dc cycling characteristics of 100 times in (a) RESET and (b) SET voltage regions at V_{READ} = 0.1V for 15 nm AVD HfO_2 1T1R RRAM cells.

tive switching behavior was observed for dc cycling of 100 times. SET and RESET voltages were measured about 1.2 and 1.6 V, respectively, indicating that the RRAM device can be operated below 2 V.

Acknowledgements This work was supported by the European Union's 2020 research and innovation programme under grant agreement No. 640073.

.

References

[1] R. Waser, and M. Aono, Nat. Mater., 6, 833 (2007).
[1] K. H. Wu, H. C. Chien, C. C. Chan, T. S. Chen, and C. H. Kao, IEEE Trans. Electron Devices, 52, 987 (2005).
[2] Memories inWireless Systems. Berlin, Germany: Springer-Verlag, 2009.
[3] Embedded Memories for Nano-Scale VLSIs. New York: Springer-Verlag, 2009.
[4] H.-S. P. Wong, H.-Y. Lee, S. Yu, Y.-S. Chen, Y. Wu, P.-S. Chen, B. Lee, F. T. Chen, and M.-J. Tsai, Proc. IEEE., 100, 1951 (2012).
[5] A. Sawa, Mater. Today, 11, 28 (2008).
[6] M. J. Yun, H.-D. Kim, S. M. Hong, J. H. Park, D. S. Jeon, and T. G. Kim, J. Appl. Phys., 115, 094305 (2014).
[7] B. J. Choi, J. J. Yang, M.-X. Zhang, K. J. Norris, D. A. A. Ohlberg, N. P. Kobayashi, G. Medeiros-Ribeiro, and R. S. Williams, Appl. Phys. A-Mater. Sci. Process., 109, 1 (2012).
[8] K. G. Young-Fisher, G. Bersuker, B. Butcher, A. Padovani, L. Larcher, D. Veksler, and D. C. Gilmer, IEEE Electron Device Lett., 34, 750 (2013).
[9] S. Long, L. Perniola, C. Cagli, J. Buckley, X. Lian, E. Miranda, F. Pan, M. Liu, and J. Suñé, Sci. Rep., 3, 2929 (2013).
[10] E. A. Miranda, Ch. Walczyk, Ch. Wenger, Th. Schroeder, IEEE Electron Dev. Lett., 31, 609 (2010).
[11] Ch. Walczyk, D. Walczyk, Th. Schroeder, Th. Bertaud, M. Sowinska, M. Lukosius, M. Fraschke, D. Wolansky, B. Tillack, E. Miranda, and C. Wenger, IEEE Trans. Electron Devices, 58, 3124 (2011).
[12] Q. Liu, W. Guan, S. Long, R. Jia, M. Liu, and J. Chen, Appl. Phys. Lett., 92, 012117 (2008).
[13] L.M. Procel, L. Trojman, J. Moreno, V. Maccaronio, F. Crupi, R. Degraeve, L. Goux, E. Simoen, J. Appl. Phys., 114, 074509, 201